Biochimica et Biophysica Acta, 769 (1984) 585–595
Elsevier

BBA 71998

EFFECTS OF POLYPEPTIDE-PHOSPHOLIPID INTERACTIONS ON BILAYER REORGANIZATIONS

RAMAN SPECTROSCOPIC STUDY OF THE BINDING OF POLYMYXIN B TO DIMYRISTOYLPHOSPHATIDIC ACID AND DIMYRISTOYLPHOSPHATIDYLCHOLINE DISPERSIONS

ERNEST MUSHAYAKARARA and IRA W. LEVIN *

Laboratory of Chemical Physics, National Institute of Arthritis, Diabetes, and Digestive and Kidney Diseases, National Institutes of Health, Bethesda, MD 20205 (U.S.A.)

(Received May 27th, 1983)

Key words: Protein-lipid interaction; Raman spectroscopy; Polymyxin B; Phosphatidic acid bilayer; Dimyristoylphosphatidylcholine; Phase transition; Bilayer organization

The interactions of the antibiotic polymixin B, a polycationic cyclic polypeptide containing a branched acyl side chain, with dimyristoylphosphatidylcholine (DMPC) and dimyristoylphosphatidic acid (DMPA) bilayers were investigated by Raman spectroscopy for a wide range of lipid/polypeptide mole fractions. Temperature profiles, constructed from peak height intensity ratios derived from the lipid methylene C-H stretching and acyl chain C-C stretching mode regions, reflected changes originating from lateral chain packing effects and intrachain *trans/gauche* rotamer formation, respectively. For DMPC/polymyxin B bilayers the temperature dependent curves indicate a broadening of the gel-liquid crystalline phase transition accompanied by an approx. 3 C deg. increase in the phase transition temperature from 22.8°C for the pure bilayer to 26°C for the polypeptide complex. For a 10:1 lipid/polypeptide mole ratio the temperature profile derived from the C-C mode spectral parameters displays a second order/disorder transition, at approx. 35.5°C, associated with the melting behavior of approximately three bilayer lipids immobilized by the antibiotic's charged cyclic headgroup and hydrophobic side chain. For the 10:1 mole ratio DMPA/polypeptide liposomes, the temperature profiles indicate three order/disorder transitions at 46, 36 and 24°C. Pure DMPA bilayers display a sharp lamellar-micellar phase transition at 51°C.

Introduction

Polymyxin B sulfate represents one of several cyclic polypeptides distinguished by an acyl side chain and five positively charged diaminobutyric acid residues [1,2]. This polypeptide antibiotic displays a specificity to Gram-negative bacteria, generally targeting negatively charged lipids at the cell surface and in the cytoplasmic membrane [2–4]. Indeed, this specific affinity to negatively charged lipids has been effectively applied toward mapping the surface phospholipid composition of mammalian cells [5]. The amphiphilic nature of polymyxin B, reflected by the hydrophilic heptapeptide ring moiety and the hydrophobic acyl chain, presents a useful model system for assessing and delineating the predominant contributions to lipid-polypeptide interactions in membrane assemblies. In particular, comparisons between the interactions exhibited by polymyxin B with membrane bilayers composed of either acidic or neutral phos-

* To whom correspondence should be addressed.

pholipids enhance our understanding of the general structural prerequisites required for lipid-protein associations involving both the mechanisms for insertion of membrane constituents and the architectural details of intramembrane complexes.

Among the diverse physical methods successfully employed in examining bilayer lipid-polymyxin B interactions, vibrational Raman spectroscopy provides a sensitive, noninvasive approach toward probing the structural and dynamical properties exhibited by lipid assemblies [6–8] on the 10^{-12}–10^{-13} s time scale. Other techniques utilized in elucidating polymyxin B interactions have included fluorescence polarization [9], electron paramagnetic resonance spectroscopy [9,10], electron microscopy [9] and calorimetry [11]. In the Raman technique, however, various aspects of conformational behavior involving the response of the membrane bilayer matrix to environmental perturbations may be monitored through the frequency and intensity alterations reflected by vibrational modes characteristic of specific structural regions of the lipid components. In the present discussion we emphasize the use of the methylene C-H stretching modes in the 2800–3100 cm^{-1} spectral interval and the acyl chain C-C skeletal stretching modes in the 1000–1200 cm^{-1} region of Raman spectra for generating temperature profiles for reconstituted lipid/polymyxin B multilamellar, aqueous dispersions. These temperature dependent curves specifically reflect lateral chain packing effects and intrachain *trans/gauche* rotamer formation, respectively. Raman spectra of multilamellar dispersions reconstituted with polymyxin B and bilayers of dimyristoylphosphatidic acid (DMPA), whose headgroups exist as either single or double negatively charged lipid species depending upon the pH of the assembly, and of dimyristoylphosphatidylcholine (DMPC), a zwitterionic lipid, were examined in an effort to discern the relevant electrostatic and geometrical effects leading to the development of immobilized lipids within the bilayer matrix. For the DMPC bilayers we will compare the polymyxin B system to melittin containing liposomes, a system in which both the hydrophobic and hydrophilic regions of the α-helical polypeptide immobilize bilayer lipids [7]. The general discussion will be concerned with only the intact polymyxin B decapeptide and acyl chain system; subsequent articles in this series will examine the effects of separately cleaved hydrophobic and hydrophilic fragments on bilayer behavior.

Experimental procedures

Samples of 1,2-dimyristoyl-*sn*-glycero-3-phosphocholine (DMPC) were purchased from Sigma Chemical Co. Since no contaminants were observed in the vibrational spectra of the polycrystalline material, the phospholipid was used without further purification. High purity samples of polymyxin B sulfate were commercially obtained from Sigma Chemical Co. Dimyristoylphosphatidic acid (DMPA) was procured from Avanti Polar Lipids, Inc., as the free acid in chloroform. The purity of lyophilized samples of DMPA was ascertained by thin-layer chromatographic procedures.

Sample preparation for the pure lipids consisted of first mechanically agitating aqueous dispersions (50% by weight) for 5 min, incubating the suspension for 1 h at 20°C above the primary lipid phase transition and then mechanically reshaking. The lipid/polymyxin B samples were analogously prepared with DMPC/antibiotic mole ratios of 35 : 1, 25 : 1, 10 : 1 and 5 : 1. DMPA/polymyxin B samples with a mole ratio of 10 : 1 were also prepared at pH 8, corresponding to a degree of hydrogen dissociation of about 1.5 [27]. 10–20 μl of the hydrated samples were drawn into glass capillary tubes, spun in a bench-top clinical centrifuge and sealed. The tube was then placed within a thermostatically controlled brass block, which was optically aligned in the Raman spectrometer. Prior to obtaining a temperature profile, the sample was thermally annealed.

Raman spectra were recorded at a spectral resolution of 3–4 cm^{-1} with a Spex Ramalog 6 spectrometer equipped with holographic gratings. A Coherent Model CR-12 argon ion laser provided at the sample approx. 200 MW of excitation power at 514.5 nm. Frequencies are reported to ± 2 cm^{-1}. Raman spectra were acquired with an interfaced Nicolet NIC-1180 data system. Either 10–20 or 3–4 signal averaged spectral scans were obtained for the 990–1200 cm^{-1} C-C stretching and the 2800–3100 cm^{-1} C-H stretching mode regions, respectively, at scan rates of 1 $cm^{-1} \cdot s^{-1}$. Temper-

ature profiles were generated in an ascending mode with equilibration times of 15 min between consecutive points.

Temperature profiles for the reconstituted multilamellar assemblies were constructed from the Raman peak height intensities for the I_{2940}/I_{2885} interchain disorder/order parameters and for the I_{1090}/I_{1130} intrachain *gauche/trans* rotational isomer parameters. Neither spectral deconvolution nor contour smoothing procedures were applied. Small spectral contributions to the lipid C-H stretching mode interval from polymyxin B were appropriately subtracted before constructing the temperature profiles (approx. 15% changes are involved in the corrected spectral ratios). Scattering from the peptide was negligible in the lipid C-C stretching mode region. Reference polymixin B spectra were obtained from aqueous solutions at the appropriate temperatures.

Results and Discussion

Figs. 1 and 2 display the temperature dependence of spectra in the 990–1200 cm^{-1} acyl chain C-C skeletal stretching and the 2800–3100 cm^{-1} C-H stretching mode regions, respectively. Changes in the spectral intensities and frequencies for the C-C stretching modes reflect alterations in the acyl chain *trans/gauche* distributions as the bilayer passes from the gel to liquid crystalline state [12,13]. The relevant in-phase and out-of-phase C-C stretching modes for an ordered, nearly all-*trans* chain in the low temperature gel state occur at about 1130 and 1064 cm^{-1}, respectively. As the temperature of the assembly increases, *gauche* rotamers are formed near the bilayer center at the chain termini. The introduction of intramolecular disorder is reflected by an increase in the spectral intensity at approx. 1085 cm^{-1}, the feature assigned to C-C stretching modes of *gauche* bonds. As the intensity increases in the 1088 cm^{-1} region, an intensity decrease, with a simultaneous frequency shift, occurs for the 1130 cm^{-1} feature. The intense feature at 1002 cm^{-1} is assigned to the characteristic in-plane ring deformation [14,15] of the phenylalanine residue within the cyclic headgroup moiety of the polypeptide. The weaker peak at 1032 cm^{-1} is also assigned to the phenylalanine moiety. These features were used for normalizing

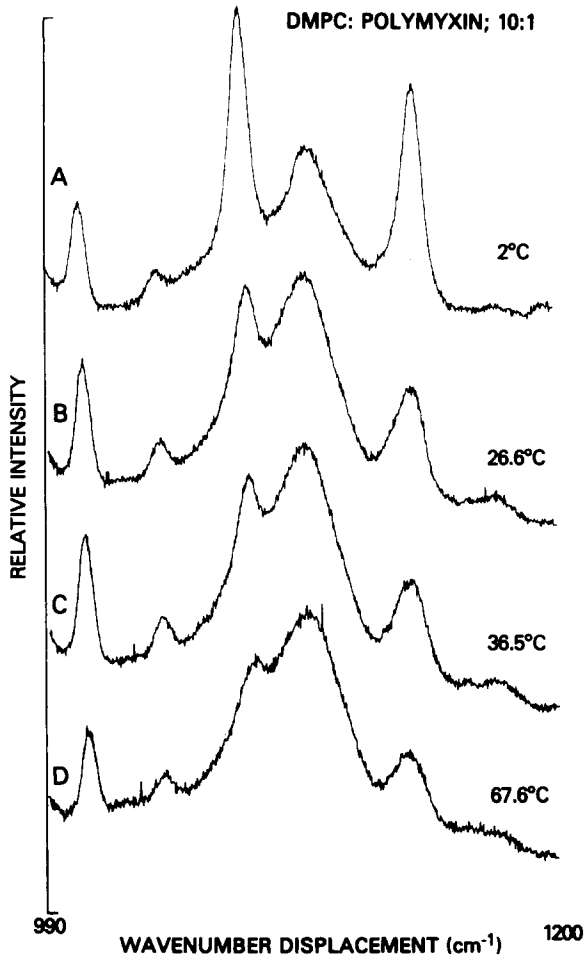

Fig. 1. Raman spectra of the 1000–1200 cm^{-1} skeletal C-C stretching mode region for a 10:1 DMPC/polymyxin B mole ratio dispersion at temperatures spanning the gel and liquid-crystalline bilayer phases.

the spectra in the computer subtraction steps in obtaining lipid spectra devoid of polypeptide contributions.

The C-H stretching region contours shown in Fig. 2 represent original spectra containing the relatively small contributions from the polymyxin B component. Although the derived temperature profiles reflect a computer subtraction of the polypeptide signals, the features of the observed spectra yield a faithful representation of the intensity changes of the bilayer lipids as a function of temperature. Since the vibrational assignments of the C-H spectral region for phospholipids have

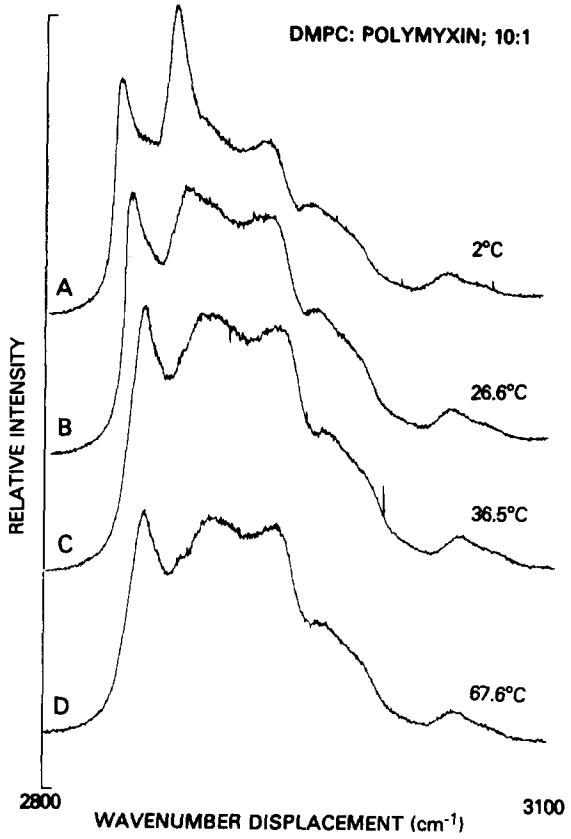

Fig. 2. Raman spectra of the 2800–3100 cm^{-1} C-H stretching mode region for a 10:1 DMPC/polymyxin B mole ratio dispersion at temperatures spanning the gel and liquid crystalline phases. The relatively minor contributions to the spectra from polymyxin B have not been subtracted.

been discussed previously [8,16–19], we only summarize the salient points. Changes in the relative intensities of the 2850, 2885 and approx. 2935 cm^{-1} modes are generally used in monitoring the packing and conformational properties of the bilayer lipid chains. These spectral transitions are assigned, respectively, to the methylene C-H symmetric stretching modes, the methylene C-H asymmetric stretching modes, and, in part, a Fermi resonance component of the acyl chain terminal methyl C-H stretching mode. As the bilayer undergoes intramolecular chain disorder during the expansion of the lattice, the intensity in the 2935 cm^{-1} region increases, while the 2885 cm^{-1} feature shifts toward higher frequencies and decreases in intensity. The latter intensity change arises from the disappearance of an underlying background which originates from a Fermi resonance interaction between the symmetric methylene C-H stretching fundamental and the manifold of binary combinations of the methylene bending modes of the extended, ordered hydrocarbon chain [20,21]. For completeness, we note that the ~2960 cm^{-1} and ~2985 cm^{-1} intervals encompass the acyl chain methyl asymmetric C-H stretching modes and the choline methyl symmetric C-H stretching modes, respectively. The choline asymmetric stretching modes appear as a doublet at slightly higher frequencies at approx. 3040 and 3060 cm^{-1}.

For multilamellar assemblies reflecting various lipid/antibiotic mole ratios, the observed changes in the characteristic C-C and C-H stretching mode regions are most easily contrasted through the use of temperature profiles in which the intra- and intermolecular bilayer order/disorder processes are followed over relatively large temperature ranges. The temperature profiles in Fig. 3, constructed from the I_{1085}/I_{1130} peak height intensity ratios, represent the induced *gauche / trans* rotomeric changes along the acyl chains. As displayed in the figure, pure DMPC bilayers, represented by the dotted line, undergo a sharp primary gel-liquid crystalline phase transition t_c at 22.8°C. Addition of polymyxin B to form a 35:1 lipid/polypeptide mole ratio results in a profile essentially identical to the pure system (data not shown). Increasing the lipid/polymixin B concentration to a 25:1 mole ratio broadens the gel-liquid crystalline phase transition interval by about 10°C and increases t_c to 26°C. A suggestion of a second order/disorder transition appears at approx. 38°C with about a 3 C deg. width. For a 10:1 lipid/polypeptide mole ratio., two order/disorder transitions are clearly discerned at 26 and 38.5°C with transition widths of 11 and 4 C deg., respectively. The primary phase transition is completely broadened for a 5:1 lipid/antibiotic mole ratio. (Transition widths were estimated from the intervals defined by the curvature of the temperature profile in the transitions region and by points establishing states A and B, respectively.)

Although it has been reported that polymyxin B does not bind to bilayers of zwitterionic species, as phosphatidylcholine, for example [4,9], the elevation and broadening of T_c, in addition to the appearance of a second, higher temperature

order/disorder transition, T_U, implies significant bilayer perturbations within the DMPC assembly. This general behavior for temperature profiles derived from Raman spectral data is similar to 25 : 1 mole ratio DMPC/melittin systems in which the charged, hydrophilic fragment (residues 20–26 of the 26 amino acid polypeptide) increase T_c for DMPC by about 1 C deg. and induces a second transition at 29°C [7]. For polymyxin B electrostatic interactions at the lipid headgroup region with the charged ring structure of the antibiotic also constrain chain melting within the bilayer matrix. For the melittin/DMPC systems the upper order/disorder transition was associated with the further fluidization of a class of immobilized, boundary lipids. With bilayers containing polymyxin B, the second transition differs, however, in that the temperature profile indicates a slight reordering of the lipid acyl chains prior to their subsequent melting. This recordering property may arise from insertion into the bilayer of the antibiotic's hydrophobic, eight carbon chain tail. Evidence supporting this correlation lies in the disappearance of the second transition in a 10 : 1 DMPC/colistin system, a very closely related heptacyclic peptide for which the antibiotic's acyl chain tail was eliminated. The details concerning the interactions of colistin and its fragments will be reported at another time (Mushayakarara and Levin, unpublished data). Following completion of the second thermal transition, the disorder of the bilayer becomes greater than that for the pure DMPC bilayer matrix. By assuming that the entire melting curve encompassing both order/disorder transitions reflects a fluidization of the lipid matrix, we estimate that about three lipid molecules are immobilized by each polymyxin B molecule. For the 5 : 1 lipid/polymyxin B mole ratio system the bilayer disorder at approx. 45°C, which is higher than the second thermal transition exhibited by the 10 : 1 DMPC/polymyxin system, is equivalent to the disorder represented by the middle of the transition (T_c) of the pure bilayer. Although the increased polymyxin B concentration significantly orders the liquid-crystalline state of DMPC through the extreme broadening of the transition, the gel state is only slightly disordered (Fig. 3).

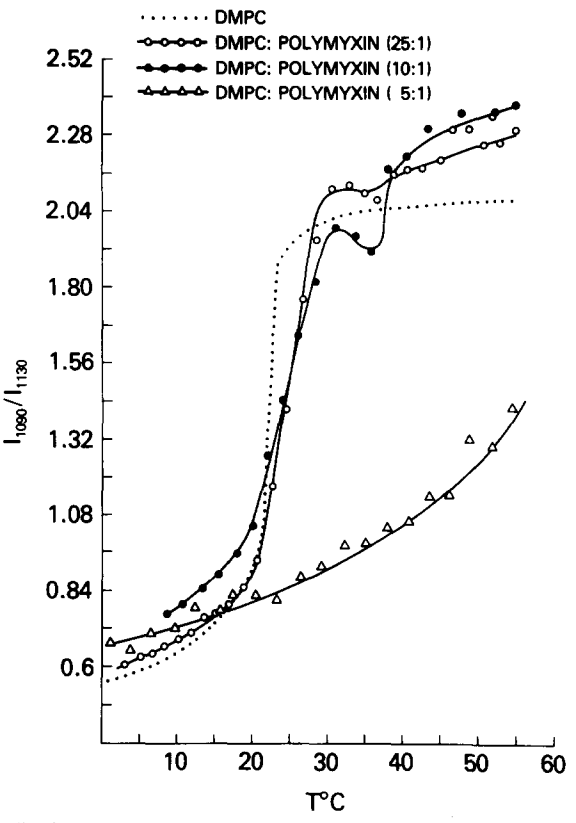

Fig. 3. Temperature profiles for DMPC/polymyxin B recombinants using the $I_{1090\,cm^{-1}}/I_{1130\,cm^{-1}}$ (I_{gauche}/I_{trans}) peak height intensity ratios as indices.

Fig. 4 presents the temperature profiles for the DMPC/polymyxin B system derived from the peak height intensity parameters I_{2940}/I_{2885}, or $I_{disorder}/I_{order}$, observed in the C-H stretching region. The increase in this parameter, as the system passes from the gel to the liquid-crystalline state, monitors changes in the lipid chain lateral packing characteristics. For the 35 : 1 lipid/polymyxin B system (data not shown), T_c remains unchanged, as in the C-C stretching region profile, except that the transition interval is broadened to about 4 C deg. as compared to approx. 1.5 C deg. broadening in the former profile. t_c increases to 26°C, with a 9 C deg. transition interval in the 25 : 1 lipid/antibiotic system. Increasing the lipid/polypeptide mole ratio to 10 : 1 leaves t_c invariant at 26°C, but increases the transition width to about 12 C deg. As in the profiles reflecting the C-C stretching region, the 5 : 1 lipid/polymyxin B system exhibits a nearly completely broadened transition. In con-

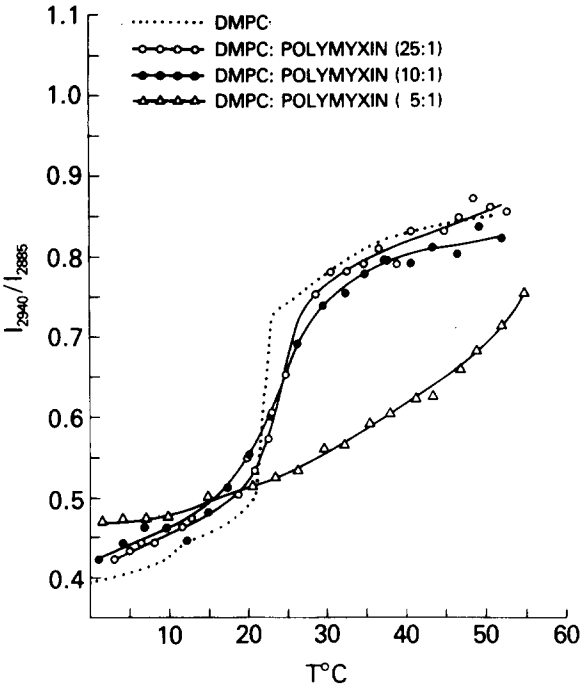

Fig. 4. Temperature profiles for DMPC/polymixin B recombinants derived from the Raman spectral $I_{2940\,cm^{-1}}/I_{2885\,cm^{-1}}$ peak height intensity ratios. Profiles were constructed from spectra corrected for polymyxin B contributions.

trast to the profiles based upon intramolecular order/disorder parameters, the profiles derived from the C-H stretching mode intensities do not exhibit the second, high temperature transition. Further, the liquid-crystalline state of the 25 : 1 system exhibits about the same disorder as the pure DMPC bilayer. The liquid-crystalline lateral chain-chain disorder for the 10 : 1 system is perhaps slightly ordered compared to the pure and 25 : 1 liposomes. For the gel state the lattice disorder increases proportionately for increasing polymyxin B concentrations. For the DMPC/melittin systems [7,22] only the C-H stretching mode profiles for intact melittin displayed the two thermal transitions at higher peptide concentrations; neither the hydrophobic nor hydrophilic fragment alone induced the higher temperature order/disorder transition. For polymyxin B we surmise that once the lipid lattice packing arrangements are sufficiently disordered by the electrostatic binding of the polar heptapeptide disk to the lipid headgroup region, the insertion of the antibiotic's acyl chain into the bilayer fails to disrupt further the lateral lipid chain organization. The hydrophobic interaction between the lipid acyl chains and the antibiotic tail leads, however, first to a slight intrachain ordering and then to increased *gauche / trans* isomerization after the melting of the immobilized lipids. The thermal transition parameters for the DMPC/polymyxin system are summarized in Table I.

The interaction of polymyxin B with negatively charged dimyristoylphosphatidic acid (DMPA) lipid bilayers is distinctly different from the effects discussed above for the zwitterionic DMPC bilayers. For a DMPA/polymyxin B mole ratio of 10 : 1 the characteristic temperature profile derived from the acyl chain *gauche / trans* isomerization parameters appears in Fig. 5. The dotted line in the figure represents the sharp phase transition for DMPA from an ordered gel state to a disordered micellar state. This lamellar-micellar transition for

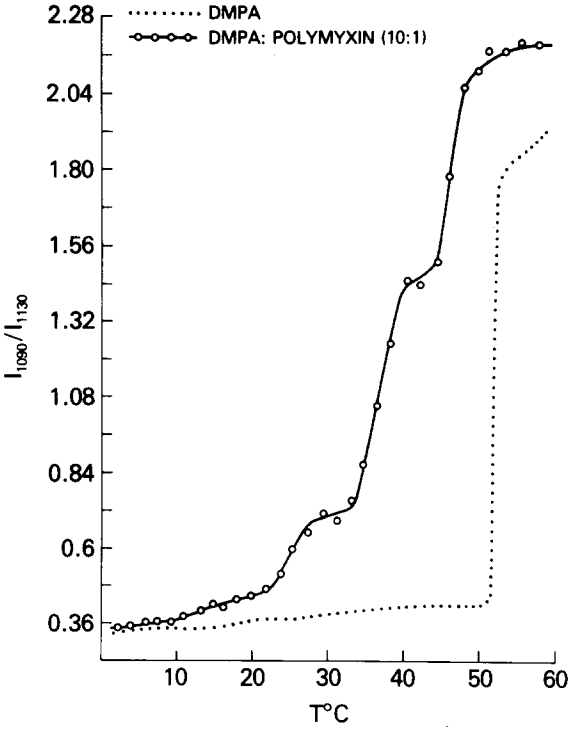

Fig. 5. Temperature profile for a 10 : 1 DMPA/polymyxin B mole ratio dispersion derived from the $I_{1090\,cm^{-1}}/I_{1130\,cm^{-1}}$ peak height intensity ratios. The dashed line represents the profile for a pure DMPA system.

TABLE I

SUMMARY OF THE ORDER-DISORDER TRANSITIONS FOR DMPC- AND DMPA-POLYMYXIN BILAYER SYSTEMS FROM RAMAN SPECTRAL PARAMETERS.

Bilayer	Lipid/ polypeptide mole ratio	Raman Marker	t_C [a] (°C)	$t_{B\text{-}M}$ [b] (°C)	t_U [c] (°C)	t_B [d] (°C)	t_A [e] (°C)
DMPC		C-C [f]	22.5 (0.5)				
DMPC/Polym	35:1	C-C	23 (1.5)				
DMPC/Polym	25:1	C-C	26 (10)		38 (3)		
DMPC/Polym	10:1	C-C	26 (11)		38.5 (4)		
DMPC/Polym	5:1	C-C	Completely broadened				
DMPC		C-H [g]	22.5 (0.5)				
DMPC/Polym	35:1	C-H	23 (4)				
DMPC/Polym	25:1	C-H	26 (9)				
DMPC/Polym	10:1	C-H	26 (12)				
DMPC/Polym	5:1	C-H	Completely broadened				
DMPA		C-C		51 (0.2)			
DMPA/Polym	10:1	C-C	46.5 (6)			36 (8)	24.5 (9)
DMPA		C-H		51 (0.2)			
DMPA/Polym	10:1	C-H	46 (9)	56 (3)		36 (5)	24 (8)
DMPC/Polym	10:1	Phe [h]	26 (7)				
DMPC/Polym	10:1	Phe		~ 55 (7)		37 (0.2)	

[a] The first value represents t_c, the bilayer gel-liquid crystalline phase transition. The value in parenthesis gives an estimate of the breadths of the transition.

[b] $t_{B\text{-}M}$ represents the bilayer-micellar phase transition.

[c] t_U represents the upper transition for DMPC/polymyxin dispersions.

[d] t_B represents the phase transition involving DMPA/polymyxin complexes bound both electrostatically and hydrophobically [10,11,24].

[e] t_A represents the phase transition involving DMPA/polymyxin complexes bound only hydrophobically [10,11,24].

[f] C-C implies use of I_{gauche}/I_{trans} peak height intensity ratios for construction of the temperature profile.

[g] C-H implies use of $I_{2940\,cm^{-1}}/I_{2885\,cm^{-1}}$ peak height intensity ratios for construction of the temperature profile.

[h] Phe implies the use of the peak height intensities (in arbitrary units) of the 1002 cm^{-1} phenyl ring distortion of the phenylalanine residue within the polymyxin headgroup.

DMPA will be discussed in greater detail later (Mushayakarara, E. and Levin, I.W., unpublished data), but at the present we note that the correspondance with a micellar state is made on the basis of the C-H stretching region spectra and temperature profiles of DMPA with those for 1-stearoyl- and 1-palmitoyllysophosphatidylcholine assemblies [19,23]. The profile in Fig. 5 for the 10:1 DMPA/polypeptide system displays the analogous three phase transitions observed by Galla and Trudell [10] by electron paramagnetic resonance spectroscopy in a 4 mol% polymyxin/DPPA liposomal system. Table I also summarizes the transition temperature data determined by Raman spectroscopy for the DMPA liposomes. The three thermal transitions at 46.5, 36 and 24.5°C exhibit widths of 6, 8 and 9 C deg., respectively. The respective transition temperatures are identified in Table I by t_c, t_B and t_A, respectively. In a series of papers by Sixl and Galla [10,11,24] the interaction of polymyxin B with charged bilayers was postulated to lead to domain formation through lateral phase separations. Their model consists of an inner core in which polymyxin B is bound hydrophobically and electrostatistically to the lipid bilayer. This complex is presumably surrounded by an annular ring of polymyxin B bound only hydrophobically to the lipid acyl chains through the antibiotic's hydrocarbon tail. The entire cluster is immersed within a free phosphatidic

acid bilayer matrix. The highest temperature transition observed at 46.5°C in Fig. 5, compared to 51°C for pure DMPA, corresponds to the acyl chain melting of the slightly perturbed bulk matrix lipid. From the amplitudes of the two lower thermal transitions derived from the Raman data, we estimate that approx. six lipids are bound to polymyxin at the pH of these experiments (pH = 8). The number of bound lipids at this mole fraction agrees well with the EPR results determined at pH = 9 for DPPA/polymyxin B liposomes [10]. (Transition temperatures differ between the Raman and EPR experiments, however, because of the pH change [10].) Calorimetric studies [11] indicate that at low ionic strengths, the lowest temperature phase transition, our T_A, consists of a superposition of a sharp component upon a broad peak. The gradual increase in intramolecular chain disorder discerned in Fig. 5 between 10 and 22°C,

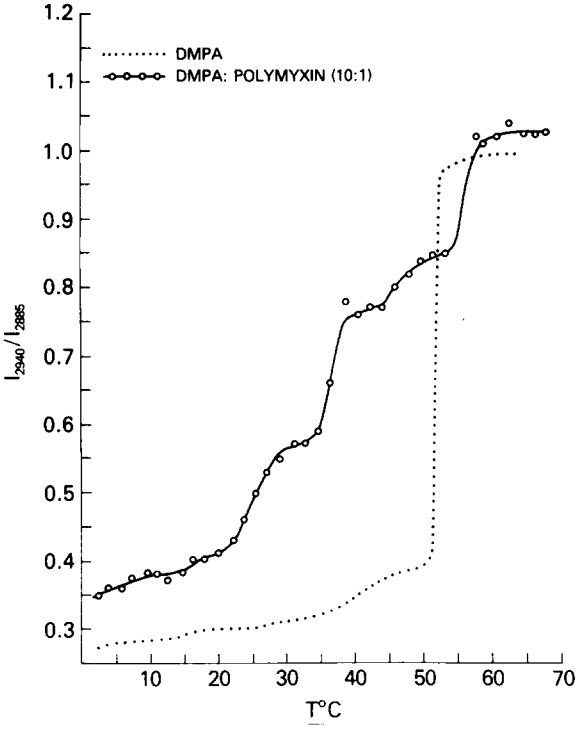

Fig. 6. Temperature profile for a dispersion of a 10:1 DMPA/polymyxin B mole ratio derived from $I_{2940\,cm^{-1}}/I_{2885\,cm^{-1}}$ peak height intensity ratios. The temperature profile was constructed from spectra for which the minor contributions from polymyxin B have been subtracted. The dashed line represents the profile for a pure DMPA system.

prior to the lowest thermal transition, may be related to the thermal characteristics associated with the broad calorimetric component.

The phase separation characteristics of the DMPA/polymyxin B system are also observed in the Raman profiles based upon the C-H spectral region parameters reflecting lateral chain-chain interactions (Fig. 6). Compared to pure DMPA at low temperatures (approx. 10°C), the polymyxin B containing liposomes exhibit considerable interchain disorder. The lowest thermal transition T_A, corresponding to the melting of the domain of lipids hydrophobically bound to polymyxin B, occurs at 24°C, in agreement with the C-C stretching region profile. The hydrophobically and electrostatically bound polymyxin B/lipid complex melts at 36°C, while the bulk lipid fluidization occurs at 46°C, again in agreement with the C-C region temperature curve. For the C-H spectral profile, however, the amplitude of the 46°C transition is significantly less in relation to the two lower transitions than that observed in the C-C curve in Fig. 5. Further, a fourth transition occurs at 56°C, an increase of 5 C deg. above the sharp 51°C transition observed for pure DMPA. We attribute the 56°C transition in the DMPA/polymyxin B system to a bilayer-micellar transition. In contrast to the lamellar-micellar phase transition for pure DMPA in which the bilayer phase is quite ordered (Figs. 5 and 6) below the transition, the bilayer phase becomes relatively disordered in the polymyxin B containing liposomes just below the transition to the micellar state. For example at 50°C, the intermolecular order is approximately 70% of that in the micellar phase, while the intramolecular *gauche/trans* ratio for the micellar lipids exceeds that of the micellar state of pure DMPA. Fig 7 depicts the C-H stretching region spectra for the DMPA/polymyxin (10:1) system at a temperature in the low temperature gel state (10.8°C), in the middle of the lowest phase transition (25.5°C), in the middle of the phase transition involving the hydrophobically and electrostatically bound polymixin B (36.9°C), after the fluidization of the bulk bilayer lipid (50°C) and in the micellar state (70.8°C). Note, in particular, the characteristic difference of the liquid-crystalline bilayer and micellar spectra of 50.0° and 70.8°C, respectively [19,23]. The 70.8°C C-H spectrum for the

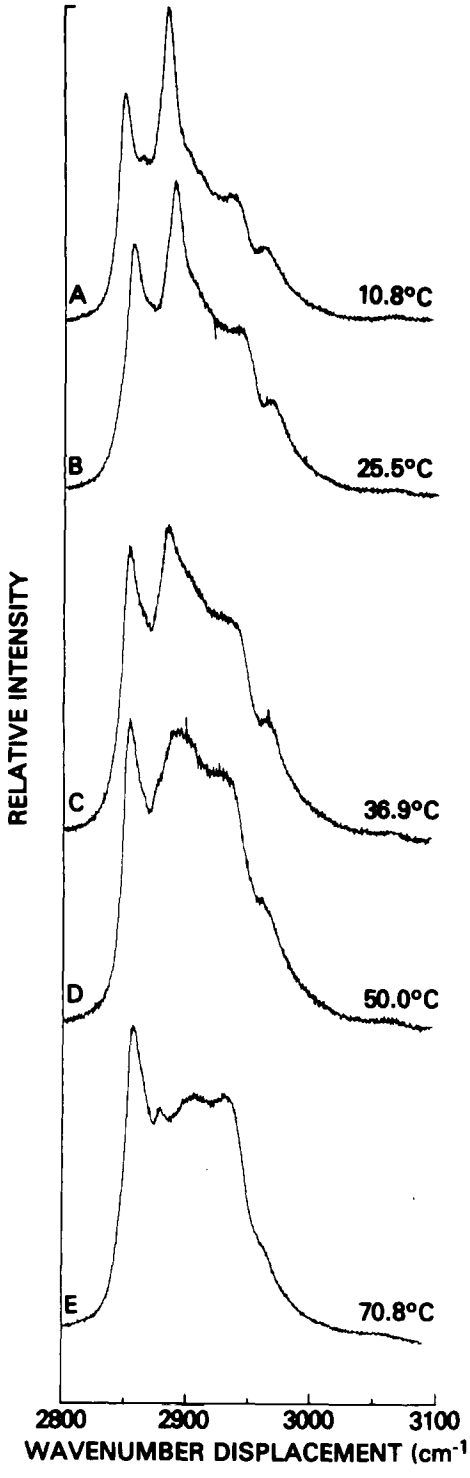

Fig. 7. Raman spectra of the 2800–3100 cm^{-1} C-H stretching mode region for a 10:1 DMPA/polymyxin B mole ratio dispersion at temperatures spanning the gel, liquid crystalline and micellar states. The minor spectral contributions from polymyxin B have not been subtracted. See text for discussion.

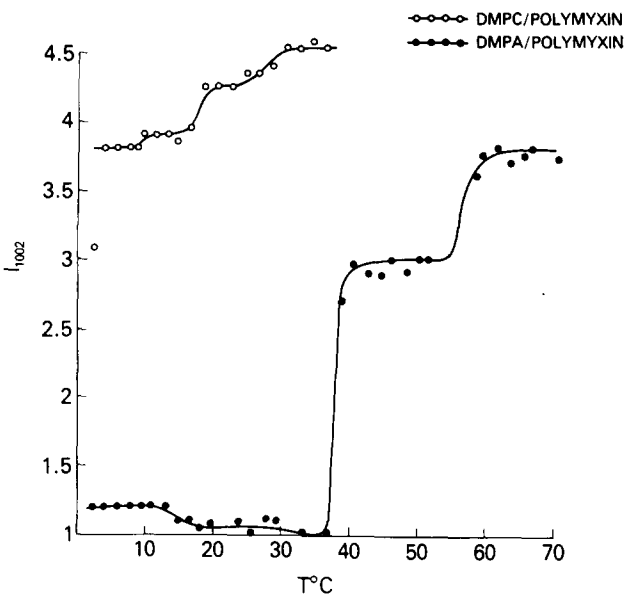

Fig. 8. Temperature profiles for 10:1 DMPC/polymyxin B and DMPA/polymyxin B mole ratio dispersions using the phenyl mode $I_{1002\,cm^{-1}}$ peak height intensities (in arbitrary units) as indices.

DMPA/polymyxin B liposomes closely matches the distinctive I_{2950}/I_{2880} and I_{2940}/I_{2880} peak height intensity ratios and spectral characteristics observed for lysophosphatidylcholine assemblies which are known to form micelles [19,23].

The intense 1002 cm^{-1} trigonal ring distortion of the phenyl group of the phenylalanine residue within the cyclic headgroup portion of polymyxin B provides a further temperature-dependent probe for assessing the differences in polymyxin binding to either the zwitterionic or negatively charged bilayer liposomes. Fig. 8 presents the peak height intensity of the 1002 cm^{-1} feature, in arbitrary units, as a function of temperature for both DMPC/polymyxin B and DMPA/polymyxin B systems in 10:1 mole ratios. As the two systems pass through their respective phase transitions, the intensity of the 1002 cm^{-1} peak increases about 5-fold for the DMPA bilayer system in comparison to DMPC. (This increase in intensity for the

1002 cm^{-1} ring mode is not clearly indicated in the separate spectra in Fig. 1, since different ordinate expansions were used in reducing the data for the figure presentation.) For the DMPA/polymyxin B system major inflections appear in the intensity profile at 37° and approx. 55°C, which, in reference to Fig. 6, correspond to the lipid fluidization for the hydrophobically and electrostatically bound complex and to the bilayer-micellar phase transition, respectively. The profile for the DMPC/polymyxin B system yields a broad inflection centered at 26°C, corresponding to the DMPC gel-liquid crystalline transition seen in Figs. 3 and 4, and a second inflection, at approx. 17°C, for which no counterpart was observed in the temperature profiles involving C-H and C-C stretching mode parameters. The extremely sharp 36°C transition reflected by the phenyl mode intensity in the DMPA complex, in comparison to the broadened transition (5 C deg. width) determined from the lipid chain parameters (see Figs. 5 and 6), implies that a highly cooperative structural change involving electrostatic interactions between the heptapeptide rings of the antibiotic and the polar headgroups of the phosphatidic acid bilayer occurs in contrast to the less cooperative hydrophobic reorganizations arising between the acyl chains of the lipid and polypeptide. Since the phenyl mode intensity changes do not indicate headgroup structural changes at approx. 24 and 46°C, we associate these order-disorder changes observed in the profiles for DMPA/polymyxin B liposomes to reorganizations occurring predominantly among the acyl chains of the bilayer lipid.

In recent X-ray diffraction studies involving the interaction of polymyxin B with negatively charged bilayers composed of dipalmitoylphosphatidylglycerol, two lamellar phases were observed for bilayers of lipid/peptide mole ratios of 10 : 1 to 25 : 1 [25]. The two low-temperature lamellar phases represented bilayers with interdigitating and non-interdigitating chains, respectively. Although we have discussed the lower transition T_A for polymyxin B in DMPA multilayers in the context of the model for the melting of lipid chains in complexes for which the antibiotic is bound only to the lipid through hydrophobic interactions [9–11,24], we suggest that alternative interpretations involving either a second lamellar phase with interdigitated chains or a simple chain reorganization from a more ordered to a less ordered crystalline lattice subcell should also be considered. Ranck and Tocanne [25] note that the area per lipid polar headgroup, a factor important to the stabilization of specific lipid phases, is increased by polymyxin B because of its charged surface area of approx. 200 $Å^2$ [4]. Interdigitation or a change in subcell packing may then be a consequence of an increase in the headgroup expansion of the lamellar assembly through both the charge repulsions between DMPA molecules and the spreading effect of the charged ring of the polymyxin B headgroup. The amplitude of T_A in Fig. 5 is consistent with a readjustment of lateral chain parameters which allows only minimal intrachain disorder to occur; that is, T_A reflects the introduction of the least number of *gauche* isomers along the chains for the three thermal order/disorder transitions.

It is of interest to compare again the interactions of melittin with acidic phospholipids to those of polymyxin B. Fluorescence measurements on DMPA/melittin systems at pH 3.5 also suggested phase separation between lipid-polypeptide complexes and pure lipid regions [26]. Two transitions were observed, the higher one disppearing on increased concentrations of melittin. Since melittin probably inserts its hydrophobic α-helical region into the bilayer [7], the lipid chains become more laterally disordered in comparison to the lesser bilayer perturbation incurred during the insertion of only the acyl chain tail of polymyxin B. Although the low temperature state of pure DMPA bilayers, at pH 3 and 8 are quite ordered (see Fig. 6), the more severe disruption of the chain packing from the introduction of the α-helix probably precludes the appearance of a more subtle chain packing reorganization that might be evident in the gel state containing the cyclic antibiotic.

In summary, the interactions of polymyxin B with zwitterionic and acidic bilayer membranes indicate that rather different lipid-polypeptide associations are available to a charged, intrusive membrane component. With the neutral lipid DMPC species, polymyxin B slightly increases the gel to liquid-crystalline phase transition primarily through electrostatic interactions. After formation

of the liquid-crystalline state, a second order/disorder transition involving about three immobilized lipid molecules is observed in temperature profiles reflecting intrachain *gauche/trans* disorder. The slight ordering preceeding the transition is associated with an insertion into the bilayer of the hydrophobic tail region of the antibiotic. In contrast, the temperature profiles for DMPA/polymyxin B liposomes probably indicate the domain separation implied by a number of physical techniques and proposed by other authors [9–11,24]. We suggest that the lowest of the three phase transitions observed, T_A, may perhaps be related to either the formation of interdigitated chains or, more likely, to a rearrangement of the bilayer lateral chain packing parameters in which a less ordered subcell is formed. In addition, we emphasize that at high temperatures the DMPA/polymyxin B assembly undergoes a bilayer-micellar phase transition, analogous to that for the transitions observed in pure DMPA liposomes and in 1-C_{16}- and 1-C_{18}-lysophosphatidylcholine dispersions.

Acknowledgment

We thank Dr. T.J. O'Leary for illuminating and helpful discussions.

References

1 Katz, E. and Demain, A.L. (1977) Bacteriol. Rev. 41, 449–474
2 Storm, D.R., Rosenthal, K.S. and Swanson, P.E. (1977) Annu. Rev. Biochem. 46, 723–763
3 Feingold, D.S., Hsu Chen, C.C. and Sud, I.J. (1974) Ann. N.Y. Acad. Sci. 235, 480–492
4 Teuber, M. and Miller, I.R. (1977) Biochim. Biophys. Acta 467, 280–289
5 Bradley, M.P., Rayns, D.G. and Forrester, J.T. (1980) Arch. Androl. 4, 195–204
6 Levin, I.W. (1983) in Advances in Infrared and Raman Raman Spectroscopy (Clark, R.J.H. and Hester, R.E., eds.), Vol. 11, Heyden, London, in the press
7 Levin, I.W., Lavialle, F. and Mollay, C. (1982) Biophys. J. 37, 339–349
8 Gaber, B.P. and Peticolas, W.L. (1977) Biochim. Biophys. Acta 465, 260–274
9 Hartman, W., Galla, H.-J. and Sackmann, E. (1978) Biochim. Biophys. Acta 510, 124–139
10 Galla, H.-J. and Trudell, J.R. (1980) Biochim. Biophys. Acta 602, 522–530
11 Sixl, F. and Galla, H.J. (1982) Biochim. Biophys. Acta 633, 466–478
12 Spiker, R.C. and Levin, I.W. (1976) Biochim. Biophys. Acta 433, 457–468
13 Lavialle, F. and Levin, I.W. (1980) Biochemistry 26, 6044–6050
14 R.C. Lord and Yu, N.-T. (1970) J. Mol. Biol. 51, 203–213
15 Dollish, F.R., Fately, W.G. and Bentley, F.F., (1974) Characteristic Raman Frequencies of Organic Compounds, John Wiley and Sons, Inc., New York
16 Yellin, N. and Levin, I.W. (1977) Biochim. Biophys. Acta 489, 177–190
17 Spiker, R.C. and Levin, I.W. (1976) Biochim. Biophys. Acta 455, 560–575
18 Bunow, M. and Levin, I.W. (1977) Biochim. Biophys. Acta 487, 388–394.
19 Huang, C., Lapides, J. and Levin, I.W. (1982) J. Am. Chem. Soc. 104, 5926–5930
20 Snyder, R.G., Tsu, S.L. and Krimm, S. (1978) Spectrochim. Acta. 34A, 395–406
21 Snyder, R.G. and Scherer, J.R. (1979) J. Chem. Phys. 71, 3221–3228
22 Lavialle, F., Levin, I.W. and Mollay, C. (1980) Biochim. Biophys. Acta 600, 62–71
23 Wu, W., Huang, C., Conley, T.G., Martin, R.B. and Levin, I.W . (1982) Biochemistry 21, 5957–5961
24 Sixl, F. and Galla, H.-J. (1979) Biochim. Biophys. Acta 557, 320–330
25 Ranck, J.L. and Tocanne, J.F. (1982) FEBS Lett. 143, 171–174
26 Bernard, E., Faucon, J.F., Dufourcq, J., Duchesneau, L. and Pezolet, M. (1982) Biophys. J. 37, 61–62
27 Eibl, H. and Blume, A. (1979) Biochim. Biophys. Acta 553, 476–488